The Journal of Immunology

Resolvin D1 Dampens Pulmonary Inflammation and Promotes Clearance of Nontypeable *Haemophilus influenzae*

Amanda Croasdell, Shannon H. Lacy, Thomas H. Thatcher, Patricia J. Sime and Richard P. Phipps

J Immunol 2016; 196:2742-2752; Prepublished online 3 February 2016;
doi: 10.4049/jimmunol.1502331
http://www.jimmunol.org/content/196/6/2742

The Journal of Immunology is published twice each month by
The American Association of Immunologists, Inc.,
1451 Rockville Pike, Suite 650, Rockville, MD 20852

Print ISSN: 0022-1767 Online ISSN: 1550-6606.

Resolvin D1 Dampens Pulmonary Inflammation and Promotes Clearance of Nontypeable *Haemophilus influenzae*

Amanda Croasdell,[*,†] Shannon H. Lacy,[*,†] Thomas H. Thatcher,[†,‡] Patricia J. Sime,[*,†,‡] and Richard P. Phipps[*,†,‡]

Nontypeable *Haemophilus influenzae* (NTHi) is a Gram-negative, opportunistic pathogen that frequently causes ear infections, bronchitis, pneumonia, and exacerbations in patients with underlying inflammatory diseases, such as chronic obstructive pulmonary disease. In mice, NTHi is rapidly cleared, but a strong inflammatory response persists, underscoring the concept that NTHi induces dysregulation of normal inflammatory responses and causes a failure to resolve. Lipid-derived specialized proresolving mediators (SPMs) play a critical role in the active resolution of inflammation by both suppressing proinflammatory actions and promoting resolution pathways. Importantly, SPMs lack the immunosuppressive properties of classical anti-inflammatory therapies. On the basis of these characteristics, we hypothesized that aspirin-triggered resolvin D1 (AT-RvD1) would dampen NTHi-induced inflammation while still enhancing bacterial clearance. C57BL/6 mice were treated with AT-RvD1 and infected with live NTHi. AT-RvD1–treated mice had lower total cell counts and neutrophils in bronchoalveolar lavage fluid, and had earlier influx of macrophages. In addition, AT-RvD1–treated mice showed changes in temporal regulation of inflammatory cytokines and enzymes, with decreased KC at 6 h and decreased IL-6, TNF-α, and cyclooxygenase-2 expression at 24 h post infection. Despite reduced inflammation, AT-RvD1–treated mice had reduced NTHi bacterial load, mediated by enhanced clearance by macrophages and a skewing toward an M2 phenotype. Finally, AT-RvD1 protected NTHi-infected mice from weight loss, hypothermia, hypoxemia, and respiratory compromise. This research highlights the beneficial role of SPMs in pulmonary bacterial infections and provides the groundwork for further investigation into SPMs as alternatives to immunosuppressive therapies like steroids. ***The Journal of Immunology*****, 2016, 196: 2742–2752.**

Nontypeable *Haemophilus influenzae* (NTHi) is a Gram-negative, opportunistic bacterial pathogen found in the upper respiratory tract. NTHi is the most common colonizing bacterium and causes ear infections, bronchitis, and more invasive diseases such as bacteremia and pneumonia (1, 2). People with underlying lung inflammation, such as chronic obstructive pulmonary disease (COPD), cystic fibrosis, or a pre-existing infection, are particularly susceptible to infectious exacerbations, which lead to high rates of hospitalization and worsening of symptoms; NTHi is a major cause of exacerbation (3–6). NTHi is indeed the most common colonizing bacterium found in COPD patients, with the bacterial load correlating to airway inflammation, symptoms, and exacerbations (6–8). These infections are persistent and recurring, and a history of exacerbations is the single best predictor of further exacerbations (9). Although a vaccine is available for the commonly infectious *H. influenzae* type B, it does not protect against NTHi, which continues to increase in incidence (10). Furthermore, there is increased prevalence of strains with antibiotic resistance (10–12). These infections are typically persistent, with some strains acquiring drug resistance or the ability to avoid opsonization and thereby "trick" macrophages to avoid phagocytosis, resulting in the propagation and colonization of bacteria in the airways (13, 14). Multiple studies have shown that NTHi infections induce a strong and prolonged inflammatory response, characterized by influx of inflammatory cells, release of cytokines, activation of the NF-κB pathway, and initiation of TLR signaling pathways (15–18). In mice, NTHi is rapidly cleared, but inflammation persists, providing evidence for how this bacterium might induce a dysregulation of normal inflammatory responses and a failure to resolve.

Recently, endogenous lipid-derived mediators termed specialized proresolving mediators (SPMs) have been identified as key players in the resolution of inflammation (19). SPMs are derivatives of polyunsaturated fatty acids and are divided into subclasses based on their biosynthetic pathways and structures, including lipoxins, resolvins, protectins, and maresins (19). SPMs have both anti-inflammatory and proresolving actions, and it is clear that they are not immunosuppressive. These molecules act to promote a paradigm shift in immune cell function, enhancing apoptotic cell clearance, promoting production of proresolving cytokines, and inducing an alternative M2 macrophage phenotype (19–22). SPMs are effective at reducing inflammation and promoting resolution in

*Department of Environmental Medicine, University of Rochester School of Medicine and Dentistry, Rochester, NY 14642; †Lung Biology and Disease Program, University of Rochester School of Medicine and Dentistry, Rochester, NY 14642; and ‡Department of Medicine, University of Rochester School of Medicine and Dentistry, Rochester, NY 14642

ORCIDs: 0000-0001-7177-3041 (T.H.T.); 0000-0002-6428-1388 (R.P.P.).

Received for publication October 30, 2015. Accepted for publication January 3, 2016.

This work was supported in part by National Institute on Environmental Health Sciences Grant T32ES007026, National Institutes of Health Grant P30ES01247, National Institutes of Health Grant R01HL120908, National Institutes of Health Grant T32HL066988, and the PhRMA Foundation. This work was also supported in part by National Center for Research Resource Awards UL1RR024160 and 8UL1TR000042. P.J.S. was supported in part by the C. Jane Davis and C. Robert Davis Fund. The funders had no role in study design, data collection and analysis, decision to publish, or preparation of the manuscript.

The content is solely the responsibility of the authors and does not necessarily represent the official views of the National Center for Research Resources or the National Institutes of Health. S.H.L. declares that the views expressed herein are those of the author and do not reflect the official policy or position of the Department of the Army, Department of Defense, or the U.S. Government.

Address correspondence and reprint requests to Dr. Richard P. Phipps, University of Rochester Medical Center, 601 Elmwood Avenue, Box 850, Rochester, NY 14642. E-mail address: Richard_Phipps@urmc.rochester.edu

Abbreviations used in this article: AT-RvD1, aspirin-triggered resolvin D1; BAL, bronchoalveolar lavage; BALF, BAL fluid; COPD, chronic obstructive pulmonary disease; Cox-2, cyclooxygenase-2; NTHi, nontypeable *Haemophilus influenzae*; SPM, specialized proresolving mediator; veh, vehicle.

a variety of nonmicrobial models, including lung-related diseases such as COPD, asthma, and fibrosis (20, 21, 23).

Along with these proinflammatory nonmicrobial insults, there is a growing interest in evaluating the efficacy of SPMs against infectious agents. LPS is often used as a surrogate for Gram-negative bacteria, and certain SPMs—namely, lipoxins and D-series resolvins—dampen LPS-induced inflammatory cell influx and proinflammatory cytokine production (24–26). SPMs have also shown efficacy in sepsis models by promoting resolution while enhancing bacterial clearance, and ligands for the lipoxin A4 receptor (FPR2/ALX) have a protective effect against experimental sepsis (27–32). Indeed, SPMs can be used as an adjunct to antibiotics, and thereby lower antibiotic requirements or act synergistically with antibiotics for improved host responses (33, 34). There still exists, though, a major knowledge gap regarding the efficacy of SPMs in resolving pulmonary bacterial infections; this is especially critical given the susceptibility of the lung to infection. On the basis of the non-immunosuppressive nature of SPMs and their efficacy in other inflammatory lung models, we hypothesized that aspirin-triggered resolvin D1 (AT-RvD1) would attenuate NTHi-induced lung inflammation without impairing bacterial clearance. Given the high incidence of NTHi and other bacterial lung infections and their role in promoting exacerbations, this represents an important area of translational research with high clinical impact.

Materials and Methods

Materials

Mouse IL-6 (431401), IL-10 (431411), and TNF-α (430901) ELISA kits and Anti-F4/80 mouse BV421 Ab (123131) were purchased from BioLegend (San Diego, CA). Mouse CXCL1/KC ELISA kit (DY453-05) was purchased from R&D Systems (Minneapolis, MN). Collagenase (234155) was purchased from EMD Millipore (Billerica, MA). Anti-CD206 mouse Alexa Fluor 647 Ab (MCA2235A647T) was purchased from AbD Serotec (Raleigh, NC). Anti–Ly-6G (Gr-1) mouse PE Ab (553128) was purchased from BD Pharmingen (San Jose, CA). Blood agar base (70133), hemin (H9039), and b-NAD hydrate (NAD) (N3014) were purchased from Sigma-Aldrich (St. Louis, MO). Brain heart infusion (237500) and anti-CD80 mouse PerCP-Cy5.5 Ab (560526) were purchased from BD Biosciences (San Jose, CA). PGE_2 enzyme immunoassay reagents and AT-RvD1 were purchased from Cayman Chemical (Ann Arbor, MI). Secondary Western blot Abs (115-035-146, 111-035-144) were purchased from Jackson ImmunoResearch Laboratories (West Grove, PA). PBS (14200-075) was purchased from Life Technologies (Waltham, MA).

NTHi culture and growth

NTHi strain 12 (clinical isolate) was used for all infections. To culture bacteria, NTHi glycerol stock was streaked on chocolate agar plates and grown at 37˚C, 5% CO_2 for 24 h. A single colony was inoculated into supplemented brain heart infusion broth (brain heart infusion, hemin, NAD) overnight. The bacterial suspension was subcultured and then centrifuged to form a bacterial pellet. The NTHi pellet was resuspended in 1× PBS and the OD measured via spectrophotometer at a 600-nM wavelength, using OD to determine CFUs (1.00 OD = 1×10^9 CFUs).

In vivo treatment and exposures

Adult female C57BL/6J mice were purchased from The Jackson Laboratory (Bar Harbor, ME) and used at 8–10 wk of age. All animal procedures were approved and supervised by the University of Rochester University Committee on Animal Resources (UCAR protocol number 2007-127). For initial dosing experiments, mice were infected by oropharyngeal aspiration (35) with 1×10^5–10^8 CFUs of NTHi in 40 μL 1× PBS or PBS vehicle (veh) and euthanized at 6–120 h following infection. Mice were euthanized with i.p. injection of 100 mg/kg pentobarbital sodium plus 12.5 mg/kg phenytoin sodium (Euthasol; Virbac AH, Fort Worth, TX).

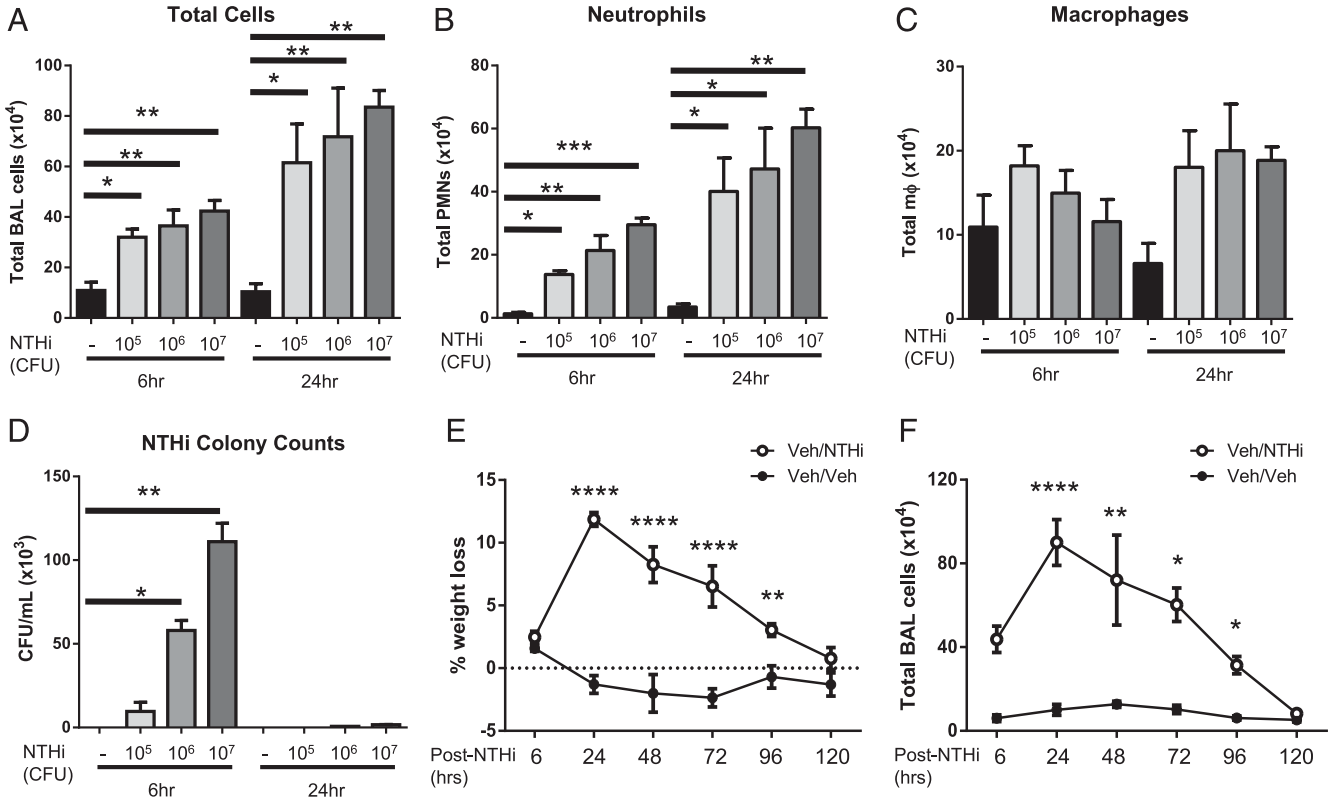

FIGURE 1. NTHi dose-dependently induces inflammation in C57BL/6 mice. Mice infected with 1×10^5–10^7 CFUs NTHi had dose-dependently increased numbers of total cells, neutrophils, and macrophages at 6 h and 24 h (**A**–**C**) post infection. NTHi infected mice also had dose-dependent levels of bacteria present in the lung at 6 h, with >90% of bacteria cleared by 24 h for all doses (**D**). NTHi-infected mice had prolonged weight loss (**E**) and prolonged influx of inflammatory cells (**F**). Statistical significance was determined by one-way ANOVA. Overall $p = 0.0014$ [(A), 6 h], $p = 0.0041$ [(A), 24 h], $p = 0.0002$ [(B), 6 h], $p = 0.0022$ [(B), 24 h], $p = 0.06$ [(C), 24 h] $p < 0.0001$ (D–F) with the Bonferroni posttest for multiple comparisons (*$p < 0.05$, **$p < 0.01$, ***$p < 0.001$, ****$p < 0.0001$), $n = 5$ mice per group.

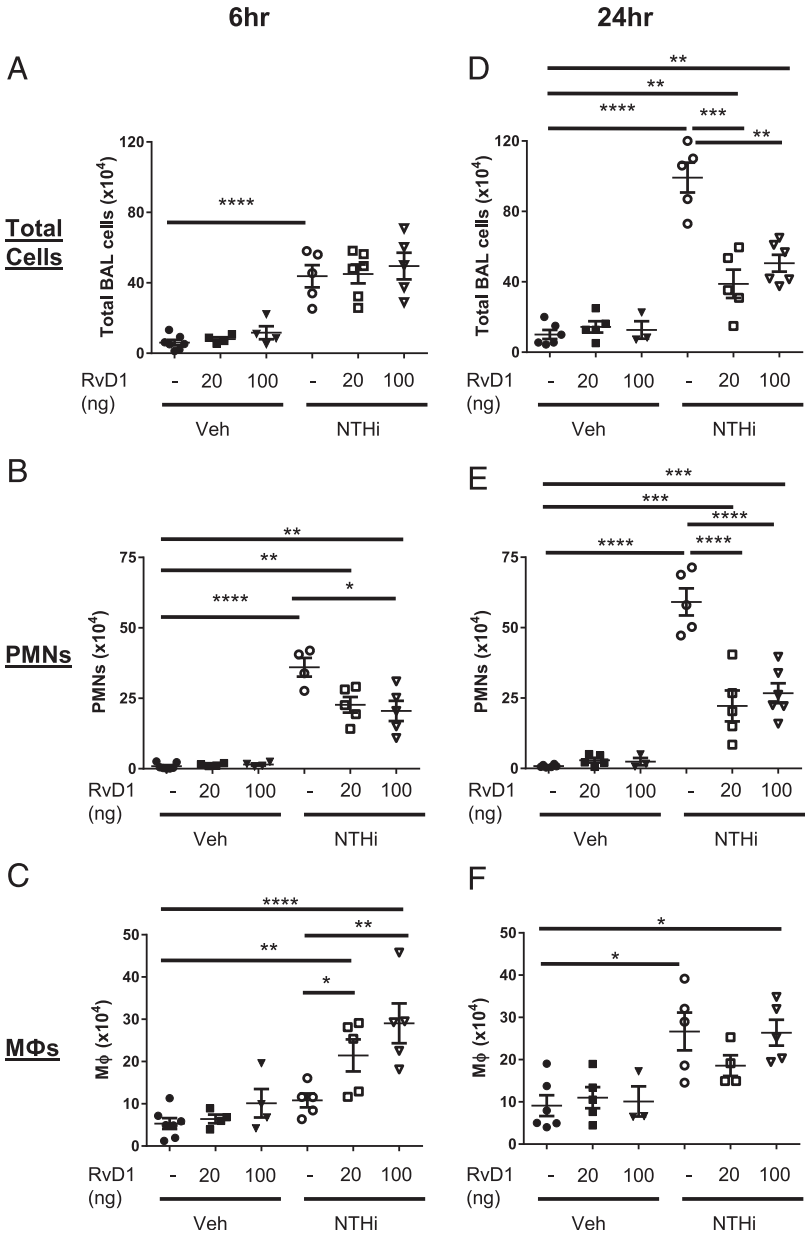

FIGURE 2. AT-RvD1 shifts the profile of inflammatory cell influx. Differential cell counts were determined from BALF of AT-RvD1 (20 or 100 ng per mouse, oropharyngeal aspiration) and/or NTHi (1×10^6 CFUs, oropharyngeal aspiration) inoculated mice. Total cell (**A** and **D**), neutrophil (**B** and **E**), and macrophage (**C** and **F**) counts were evaluated at 6 h (A–C) and 24 h (D–F). Statistical significance was determined by two-way ANOVA. Overall $p < 0.0001$, NTHi (all panels), $p = 0.0055$, AT-RvD1 (B), $p = 0.0021$, AT-RvD1 (C), $p < 0.0001$, AT-RvD1 (D and E) with the Bonferroni posttest for multiple comparisons ($^*p < 0.05$, $^{**}p < 0.01$, $^{***}p < 0.001$, $^{****}p < 0.0001$), n = 5–8 mice per group.

To determine the efficacy of AT-RvD1, mice were treated with 20 ng or 100 ng per mouse of AT-RvD1 in 40 μL 1× PBS by oropharyngeal aspiration and given a second dose 24 h later, prior to infection. As the average starting weight of the mice was 18.1 ±1.5 g (mean ±SD), this corresponded to doses of 1.1 ±0.1 mg/kg and 5.5 ±0.4 mg/kg. Mice were then infected with 1×10^6 CFUs of NTHi in 40 μL 1× PBS by oropharyngeal aspiration; 1× PBS was used as a veh control. Mice were euthanized 6–24 h following NTHi infection. Mice were weighed immediately before NTHi infection and again immediately before euthanasia. Immediately prior to euthanasia, temperature readings were also taken using a rectal thermometer. Respiratory physiology was assessed using the Harvard Apparatus Small Rodent Plethysmograph. Oxygen saturation of hemoglobin was measured using a tail clip and the Starr Life Sciences Mouse Oximeter according to the manufacturer's protocols. After all biometric readings were obtained, the mice were euthanized and tissue was harvested as described below.

Analysis of bronchoalveolar lavage fluid and lung tissue

Bronchoalveolar lavage (BAL) fluid (BALF) was collected as previously described (21). The cranial lobe of the right lung was removed to assess bacterial load. The remainder of the right lung was frozen for further analysis. Differential BALF cell counts were obtained using Richard Allen three-step staining according to the manufacturer's protocol. Total protein in BALF was determined by the bicinchoninic acid colorimetric assay (23225; ThermoScientific, Waltham, MA). Levels of IL-6, TNF-α, KC, and IL-10 cytokines in BALF were determined by ELISA. The right lung was homogenized in CW buffer (50 mM Tris-HCL, 2% SDS) using a glass bead homogenizer (Next Advance Bullet Blender, Averill Park, NY), and cyclooxygenase-2 (Cox-2) protein was analyzed by Western blotting (36). In some experiments, the lungs were inflated and fixed with 10% neutral buffered formalin without undergoing lavage. Tissues were embedded with paraffin, sectioned (5 μm), and stained for neutrophils, as described previously (21).

Assessment of bacterial load

The cranial lung lobe was homogenized in 1 ml 1× PBS. Serial dilutions were plated onto chocolate agar plates and NTHi grown at 37°C, 5% CO_2. Colonies were counted 24 h after plating.

Assessment of bacterial clearance, efferocytosis, and macrophage phenotype

Efferocytosis was performed as previously described 6 and 24 h after NTHi infection (21). To assess bacterial clearance and macrophage phenotype, mice were sacrificed 8 h after NTHi infection. BALF was obtained or the right lung lobes were removed and digested with collagenase for 30 min. Cells were collected through a cell strainer and centrifuged at 7000 × g for 10 min. RBCs were removed using 1× ACK lysis buffer. Cells from BALF and digested lung were stained with Abs against CD80, CD206, F4/80,

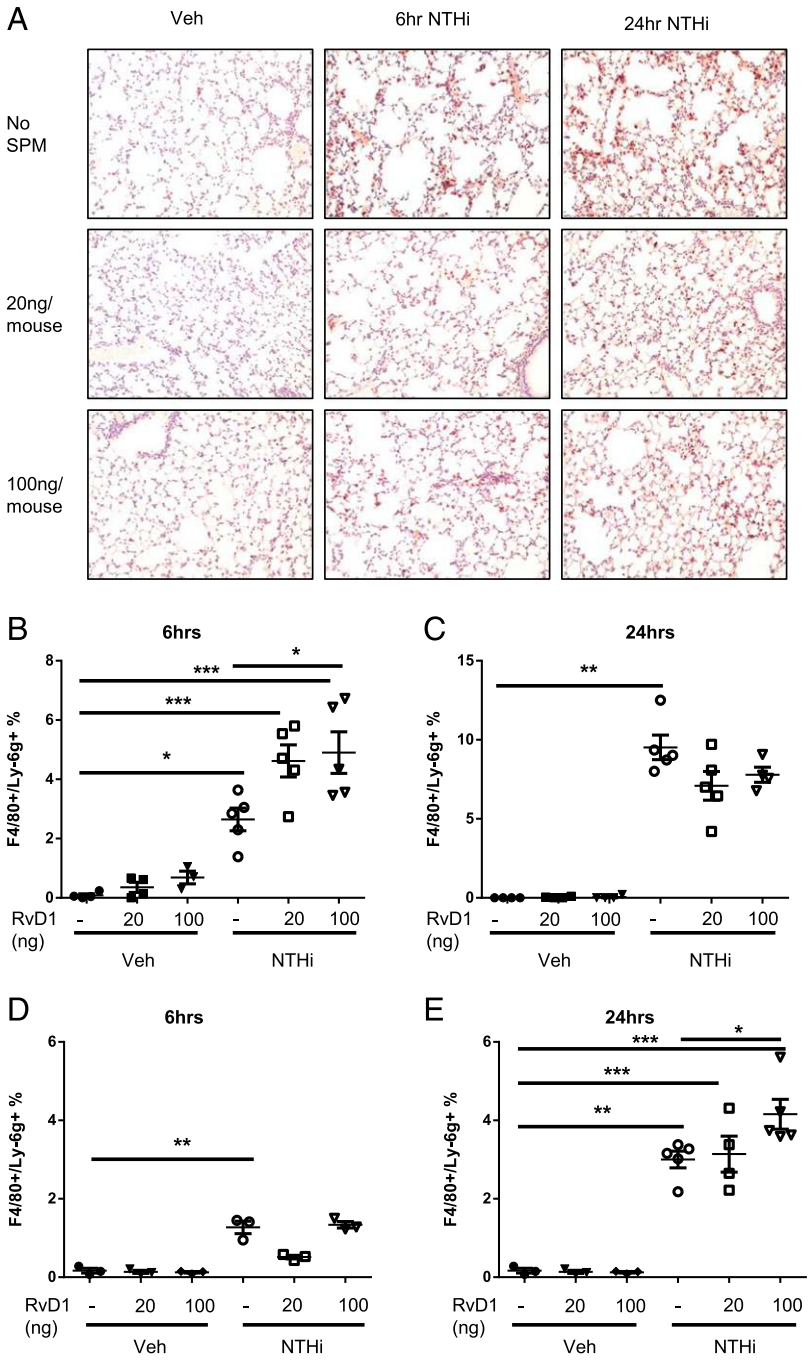

FIGURE 3. AT-RvD1 decreases neutrophil influx and promotes enhanced efferocytosis. Histological sections were taken from AT-RvD1 (20 or 100 ng per mouse, oropharyngeal aspiration) and/or NTHi (1×10^6 CFUs, oropharyngeal aspiration) inoculated mice at 6 h and 24 h and were stained for neutrophils (brown stain) and counterstained with hemotoxylin at original magnification ×40 (**A**). Efferocytosis from BAL (**B** and **C**) and collagenase digestion (**D** and **E**) at 6 h (B and D) and 24 h (C and E) were also evaluated by flow cytometry. $F4/80^+/Ly6G^+$ cells represent macrophages with ingested neutrophils. Statistical significance was determined by two-way ANOVA. Overall $p < 0.0001$, NTHi (all panels), $p = 0.0178$, AT-RvD1 (B) with the Bonferroni posttest for multiple comparisons (*$p <$ 0.05, **$p < 0.01$, ***$p < 0.001$), n = 5–8 mice per group.

CD11b, and Gr-1 for 30 min to identify cellular populations, macrophage phenotype, and bacterial clearance. For these experiments, NTHi was labeled with FITC Ab; 10 μL of a 10 mg/ml solution of FITC in DMSO was added to a suspension of NTHi and incubated in the dark for 30 min, followed by centrifugation and resuspension of the bacteria in 1× PBS, as above. Following staining, cells were fixed with 4% paraformaldehyde (15710; EMS) for 20 min. Fixed cells were then permeabilized and stained for intracellular Gr-1. Endpoints were assessed by flow cytometry.

Statistical analysis

All experiments were performed on four to nine mice per group and were repeated at a minimum of two to four independent experiments. Results are expressed as SEM. All data were normally distributed, and parametric statistical analyses were performed using a *t* test or one- or two-way ANOVA with the Bonferroni posttest correction for multiple comparisons (indicated on figures) using GraphPad Prism Software (San Diego, CA). No statistical significance was found between veh/veh versus AT-RvD1 unless indicated. In addition, AT-RvD1/veh versus NTHi groups yielded a similar level of statistical significance as veh/veh versus NTHi groups, and veh/veh versus AT-RvD1/NTHi yielded a similar level of statistical significance as veh/veh versus veh/NTHi comparisons unless otherwise indicated. The lack of statistical bar indicates that no significance was found.

Results

NTHi dose-dependently induces persistent inflammation despite rapid bacterial clearance

To characterize the timing and magnitude of NTHi-induced inflammation and infection, we first infected mice with 1×10^5–10^8 CFUs NTHi and evaluated several key markers of inflammation. Instillation of 1×10^8 CFUs caused significant tissue damage and morbidity (data not shown). At lower doses (1×10^5–1×10^7), NTHi increased the total number of inflammatory cells, neutrophils, and macrophages in BALF at both 6 and 24 h post infection in a dose-dependent manner (Fig. 1A–C). We additionally determined

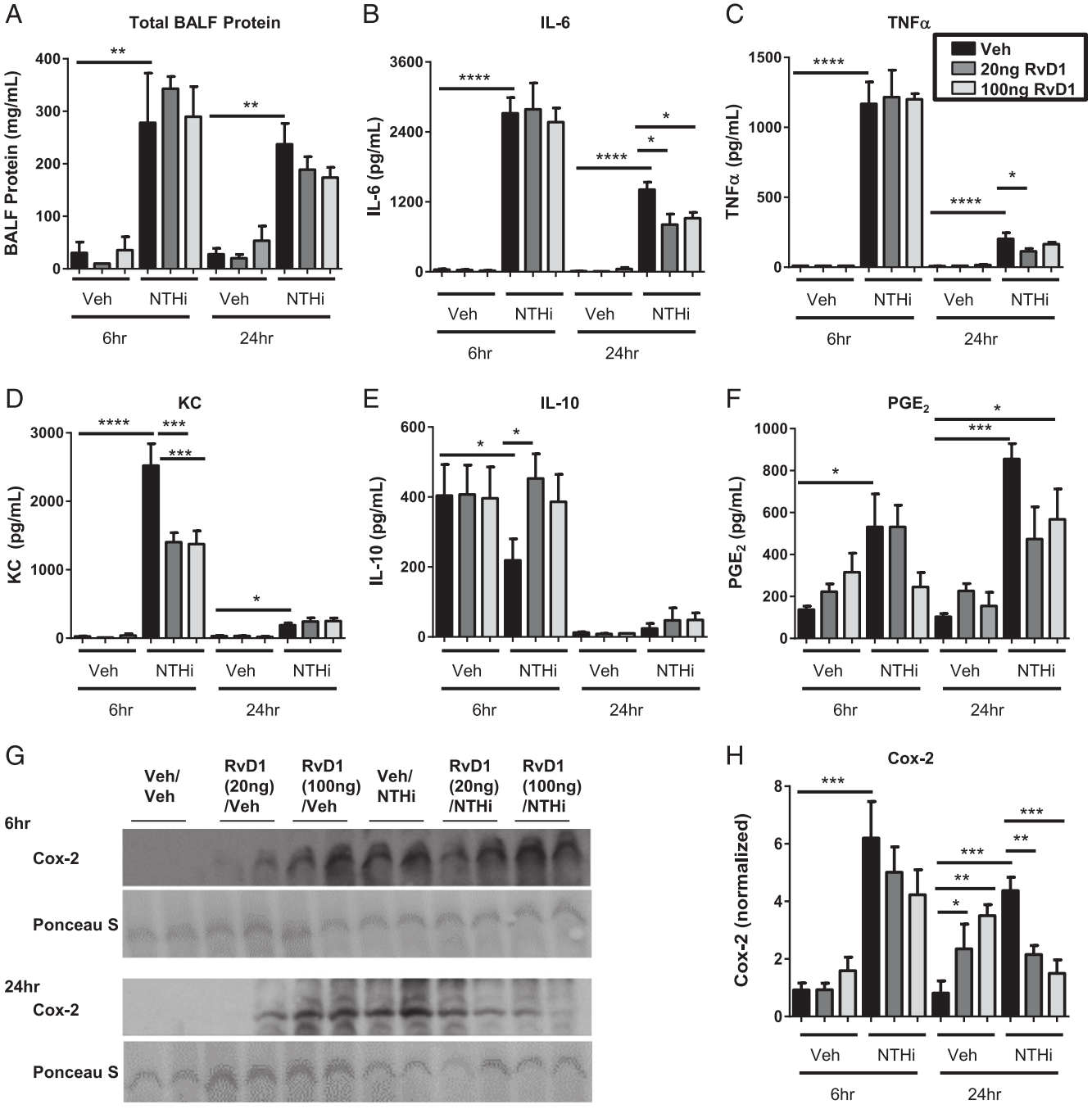

FIGURE 4. AT-RvD1 dampens production of proinflammatory cytokines. Levels of proinflammatory cytokines were measured in BALF of AT-RvD1 (veh, black bars; 20 ng per mouse, dark gray bars; or 100 ng per mouse, light gray bars, oropharyngeal aspiration) and/or NTHi (1×10^6 CFUs, oropharyngeal aspiration) inoculated mice at 6 h and 24 h. Total protein was determined by bicinchoninic acid (**A**). BALF was assessed for IL-6 (**B**), TNF-α (**C**), KC (**D**), and IL-10 (**E**). PGE_2 (**F**) expression and Cox-2 (**G** and **H**) expression were also evaluated in lung homogenates by enzyme immunoassay and Western blot, respectively (representative blots shown, densitometry on n = 4–5 mice per group). Statistical significance was determined by two-way ANOVA. Overall $p < 0.0001$, NTHi (A–D, F, and H), $p = 0.030$, AT-RvD1 [(B), 6 h], $p = 0.0257$, AT-RvD1 [(D), 24 h], $p = 0.0131$, AT-RvD1 [(H), 6 h] with the Bonferroni posttest for multiple comparisons (*$p < 0.05$, **$p < 0.01$, ***$p < 0.001$, ****$p < 0.0001$), n = 4–6 mice per group.

bacterial colony counts to evaluate clearance. In pilot testing, bacteria were distributed throughout the lung lobes in equal ratio to the lobe size (data not shown), and the right cranial (upper) lobe was used in future experiments to maintain consistency. Bacterial CFUs reflected the infective dose at 6 h; >98% of NTHi was cleared by 24 h (Fig. 1D). NTHi was never detected in the blood, spleen, or liver of infected mice (data not shown). Despite this rapid bacterial clearance and lack of bacteremia, mice infected with 1×10^6 CFUs of NTHi exhibited significant weight loss up to 96 h post infection, with recovery beginning at 48 h (Fig. 1E). Mice additionally had increasing total inflammatory cell counts 48 h post infection; by 72 h these elevated cell counts began to decrease, indicative of the initiation of resolution (Fig. 1F). These data confirm that NTHi induces persistent and prolonged lung inflammation, despite rapid bacterial clearance.

AT-RvD1 alters the NTHi-induced inflammatory cell profile and promotes efferocytosis

We next evaluated whether AT-RvD1 could attenuate excessive NTHi-induced inflammation. AT-RvD1 did not dampen initial

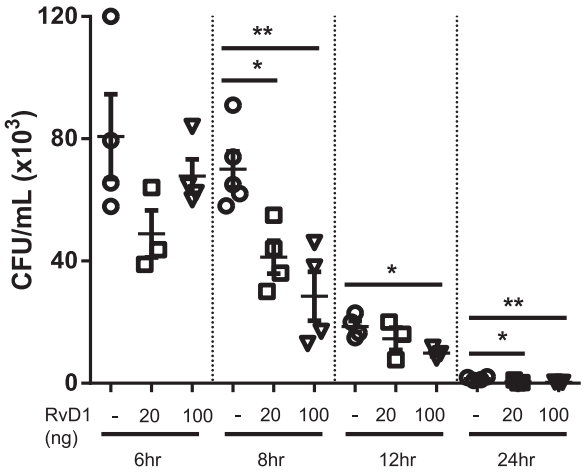

FIGURE 5. AT-RvD1–treated mice have decreased NTHi bacterial burden. Colony counts were assessed in lung homogenates 6–24 h post infection with 1×10^6 CFUs of NTHi. Statistical significance was determined at each time point by one-way ANOVA with the Bonferroni posttest for multiple comparisons ($*p < 0.05$, $**p < 0.01$), n = 3–6 mice per group.

NTHi-induced cell infiltration at 6 h, but AT-RvD1–treated mice had significantly reduced total BALF cell counts at 24 h post infection (Fig. 2A, 2D). AT-RvD1–treated mice also had decreased total polymorphonuclear neutrophil numbers at both 6 and 24 h (Fig. 2B, 2E). In contrast, AT-RvD1 increased the total number of macrophages at 6 h (Fig. 2C). However, at 24 h NTHi-infected mice showed increased total levels of macrophages; AT-RvD1–treated mice had no difference in total macrophage counts compared with NTHi-infected and veh-treated mice by 24 h (Fig. 2F).

Histological sections of lung tissue were also evaluated for neutrophil influx. NTHi-infected mice had increased neutrophil staining at 6 and 24 h post infection (Fig. 3A). These increases were strongly attenuated by AT-RvD1 treatment at both time points (Fig. 3A). Alveolar macrophages were additionally evaluated by flow cytometry to determine if enhanced efferocytosis accounted for this difference. AT-RvD1–treated mice had increased uptake of apoptotic neutrophils (early in the inflammatory response, at 6 h) in macrophages from BALF, and enhanced neutrophil uptake at 24 h by macrophages from collagenase-digested lungs (Fig. 3B–E).

AT-RvD1 temporally dampens proinflammatory cytokines and Cox-2

In addition to inflammatory cell influx, we also measured the effect of AT-RvD1 on NTHi-induced production of inflammatory cytokines in BALF. NTHi-infected mice had significantly more protein in their BALF at both 6 and 24 h, indicative of edema and inflammation (Fig. 4A). NTHi also promoted induction of proinflammatory cytokines IL-6, TNF-α, and KC (Fig. 4B–D). AT-RvD1 did not alter IL-6 or TNF-α production at 6 h but did reduce the level of KC (Fig. 4B–D). At 24 h, AT-RvD1 attenuated production of both TNF-α and IL-6 levels (Fig. 4B, 4C). KC had returned to near-background levels at 24 h, and there were no further reductions with AT-RvD1 (Fig. 4D). Along with proinflammatory cytokines, we evaluated the effect of NTHi and AT-RvD1 on the anti-inflammatory cytokine IL-10. At 6 h, NTHi reduced IL-10 expression, which was restored by AT-RvD1 treatment (Fig. 4E).

We further evaluated the effect of AT-RvD1 on PGE_2 and Cox-2 expression. Cox-2 plays multiple roles in the inflammatory process and catalyzes production of PGE_2, a PG with important roles in bacterial infections. NTHi induced strong Cox-2 expression. AT-RvD1 did not attenuate NTHi-induced Cox-2 expression at 6 h but dose-dependently dampened expression at 24 h (Fig. 4G, 4H). PGE_2 was also increased by NTHi, with trending decreases with AT-RvD1 treatment (Fig. 4F). Taken together, these data reflect the temporal regulation abilities of AT-RvD1 in reducing inflammatory cytokine and enzyme expression.

AT-RvD1 promotes bacterial clearance

A defining characteristic of AT-RvD1 is its ability to dampen inflammation and promote resolution without being immunosuppressive. To evaluate this property, we examined the effect of AT-RvD1 treatment on pulmonary bacteria levels. AT-RvD1–treated mice displayed dose-dependent decreases in bacterial colonies, consistent with bacterial clearance; this effect was evident as early as 6 h and was statistically significant by 8, 12, and 24 h (Fig. 5). AT-RvD1 did not directly act to kill NTHi, as colony counts on chocolate agar plates streaked with an NTHi or NTHi plus AT-RvD1 suspension were not significantly different (data not shown).

SPMs have been shown in nonmicrobial models of inflammation to increase phagocytic abilities of innate immune cells (20, 22, 37, 38). In particular, SPMs promote alternative M2 macrophages to mediate this enhanced phagocytosis. We hypothesized that AT-RvD1–induced decreases in bacterial CFUs were therefore due to polarization of macrophages to an M2 phenotype, which thereby mediated enhanced clearance of NTHi. Macrophages obtained by both BAL and lung collagenase digestion from AT-RvD1–treated mice had a reduced ratio of proinflammatory M1 macrophages (CD80) to proresolving M2 macrophages (CD206), compared with NTHi-infected mouse macrophages (Fig. 6A, 6E). This finding indicates a shift toward alternative M2 macrophages in AT-RvD1–treated mice. We further evaluated phagocytosis of NTHi by M1 macrophages, M2 macrophages, and neutrophils. Mice were instilled with fluorescently labeled NTHi, and double-stained macrophages and neutrophils were analyzed by flow cytometry. AT-RvD1 treatment induced no difference in NTHi phagocytosis by $CD80^+$ macrophages or by neutrophils, but $CD206^+$ macrophages had a dose-dependent increase in NTHi uptake with AT-RvD1 treatment (Fig. 6B–D, F–H).

AT-RvD1 protects health outcomes in NTHi-infected mice

Along with dampened inflammation and enhanced bacterial clearance, we investigated whether AT-RvD1 could improve the general health of infected mice. NTHi-infected mice exhibit a trend toward weight loss as early as 6 h post infection, with significant (≤15%) weight loss at 24 h (Fig. 7A, 7B). The mice also exhibit a significant 1.5°C drop in body temperature 6 h post infection; normal body temperature was restored by 24 h (Fig. 7C, 7D). AT-RvD1 treatment protected the mice from both weight loss and hypothermia, thereby preventing them from going into shock (Fig. 7A–D). NTHi-infected mice also had altered respiratory physiology, with increased respiratory rates and decreased tidal volume at 24 h, indicative of respiratory distress (Fig. 8A–D). NTHi-infected mice further exhibit a dramatic drop in the O_2 saturation of hemoglobin, comparable to that seen in humans who require mechanical ventilation (Fig. 8E, 8F). These alterations to respiratory physiology and O_2 saturation were dose-dependently rescued by AT-RvD1 treatment, restoring respiratory health (Fig. 8A–F). These results demonstrate the strong therapeutic potential of AT-RvD1 against NTHi infection.

Discussion

SPMs represent a novel class of non-immunosuppressive small lipid molecules with high clinical potential for treatment of

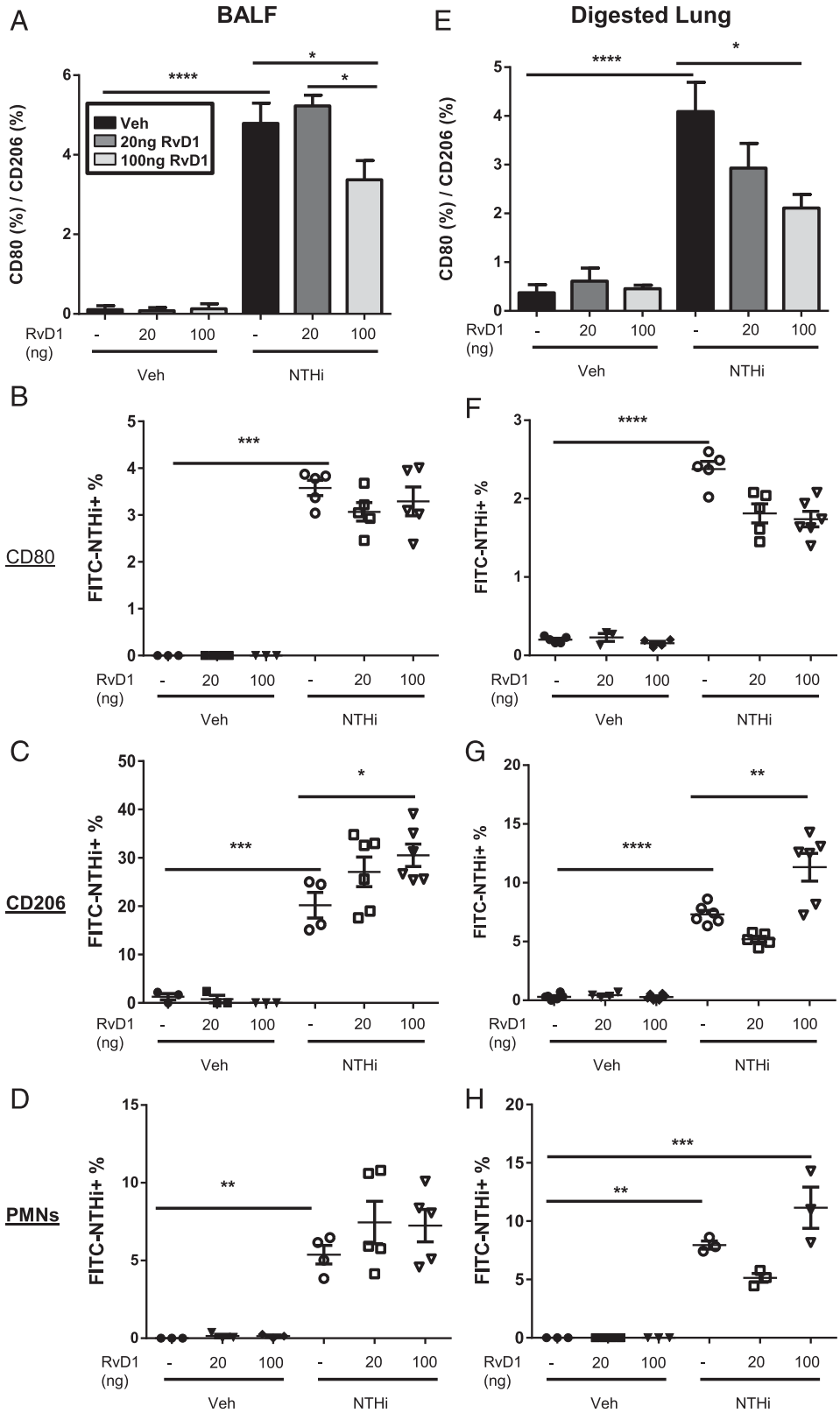

FIGURE 6. AT-RvD1 promotes M2 macrophages to mediate NTHi clearance. Mice were treated with AT-RvD1 (veh, black bars; 20 ng per mouse, dark gray bars; or 100 ng per mouse, light gray bars, oropharyngeal aspiration) and/or NTHi (1×10^6 CFUs, oropharyngeal aspiration) for 8 h. Macrophages and neutrophils were obtained from BAL (**A**–**D**) and collagenase digestion (**E**–**H**). Macrophage phenotype was assessed by flow cytometry (A and E). Uptake of NTHi by $CD80^+$ macrophages, $CD206^+$ macrophages, and neutrophils was also assessed by flow cytometry in BAL (B–D) and collagenase-digested lungs (F–H). Statistical significance was determined by two-way ANOVA. Overall $p < 0.0001$, NTHi (all panels), $p = 0.0288$, AT-RvD1 (A), $p = 0.0018$, AT-RvD1 (F), $p < 0.0001$, AT-RvD1 (G), $p = 0.0032$, AT-RvD1 (H) with the Bonferroni posttest for multiple comparisons ($^*p < 0.05$, $^{**}p < 0.01$, $^{***}p < 0.001$, $^{****}p < 0.0001$), n = 3–6 mice per group.

inflammatory diseases. In this article, we have shown that AT-RvD1 is effective at dampening NTHi-induced lung inflammation, while still promoting bacterial clearance. AT-RvD1–treated mice had reduced inflammatory cell influx, with a higher macrophage/neutrophil ratio and increased efferocytosis, compared with NTHi-infected mice receiving veh treatment. AT-RvD1 attenuated levels of proinflammatory cytokines and Cox-2 expression while preventing decreases in anti-inflammatory cytokines. Critically, these anti-inflammatory effects did not impair bacterial clearance, and AT-RvD1–treated mice had fewer NTHi CFUs. This decreased bacterial burden was mediated by an increase in M2 macrophages, which had enhanced bacterial phagocytosis. Overall, AT-RvD1–treated mice had less weight loss, less hypothermia, improved respiratory physiology, and a smaller drop in

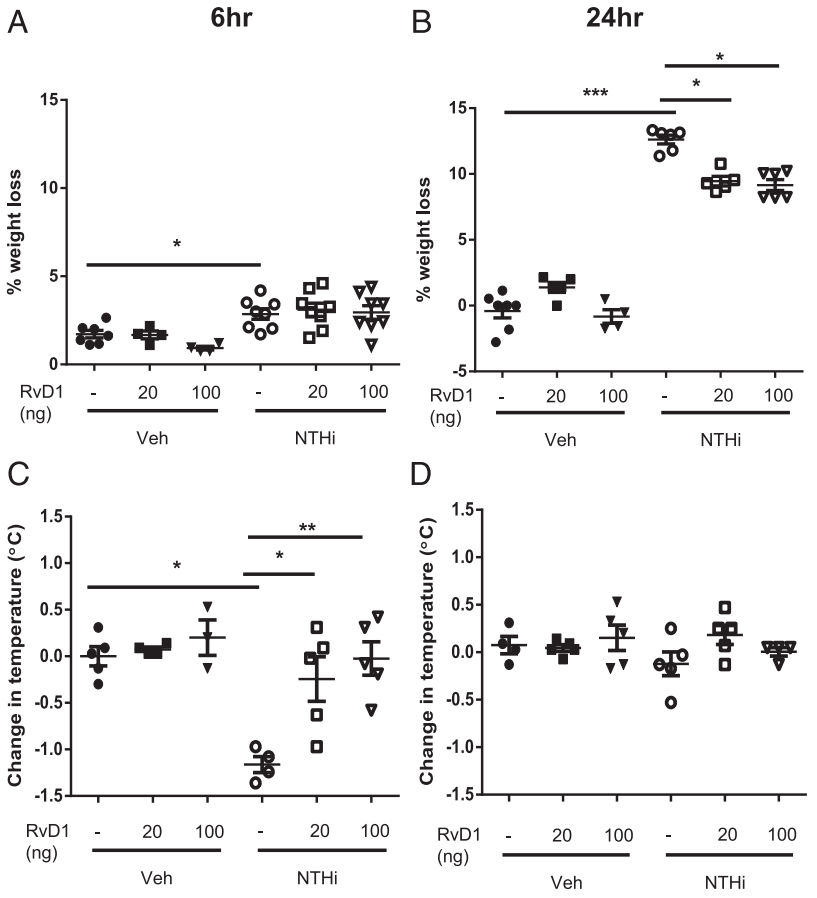

FIGURE 7. AT-RvD1 dampens NTHi-induced weight loss and hypothermia. Mice inoculated with AT-RvD1 (20 or 100 ng per mouse, oropharyngeal aspiration) and/or NTHi (1×10^6 CFUs, oropharyngeal aspiration) were weighed immediately before infection and at time of sacrifice at 6 and 24 h (**A** and **B**). In addition, the core temperature was recorded prior to euthanasia at 6 and 24 h (**C** and **D**). Statistical significance was determined by two-way ANOVA. Overall $p < 0.0001$, NTHi (A–C), $p = 0.0006$, AT-RvD1 (B), $p = 0.0019$, AT-RvD1 (C) with the Bonferroni posttest for multiple comparisons ($*p < 0.05$, $**p < 0.01$, $***p < 0.001$), n = 3–6 mice per group.

O_2 saturation, indicating less hypoxemia. These effects underscore the clinical therapeutic potential of AT-RvD1 for NTHi infection.

In each of our observed endpoints, all NTHi-infected mice mounted an initial inflammatory response, but the AT-RvD1–treated mice had more rapid clearance of NTHi and resolution of inflammation. At 6 h post infection, in the early stages of bacterial clearance, AT-RvD1 dampened KC, a cytokine that promotes neutrophil recruitment, contributing to decreased levels of neutrophils in AT-RvD1–treated lungs. However, AT-RvD1 did not dampen levels of IL-6 and TNF-α until 24 h. These cytokines are important for initial inflammatory responses, with TNF-α particularly contributing to bacterial phagocytosis and killing. This same effect was seen in inflammatory cell influx, wherein AT-RvD1 did not halt inflammatory cell influx, but shifted the cellular profile to promote an early increase in macrophages and a faster clearance of neutrophils. This regulation of cytokines at different time points is key for several reasons. First, AT-RvD1 does not broadly block all cytokine signaling, distinguishing SPMs from other strictly anti-inflammatory therapies. This nonimmunosuppressive nature is further seen as SPMs increase macrophage influx, enhance efferocytosis, and increase the phagocytic abilities of macrophages (20–22, 25, 33, 39). Second, AT-RvD1 decreases in KC levels early on demonstrate that SPMs can preferentially regulate early cytokine release to jump-start resolution. Third, endogenous resolution of NTHi-induced inflammation is slow, occurring days after bacterial clearance. AT-RvD1, however, enhances natural resolution, more rapidly clearing apoptotic cells and dampening proinflammatory cytokine release. These data highlight that SPMs do not suppress immune cell function but instead promote a shift in macrophage functional activities to speed the resolution process.

Along with temporal regulation of proinflammatory cell influx and cytokines, SPMs are also capable of shifting cytokine production to promote enhanced levels of anti-inflammatory or proresolving cytokines. SPMs are derived from ω three and ω six fatty acids, precursors that can undergo lipid class switching to produce both pro- and anti-inflammatory molecules in a temporal manner and under different stimuli (40). This feature is highlighted by our results with Cox-2; although AT-RvD1 partially inhibited the increased expression of Cox-2 in NTHi-treated mice at 24 h, it paradoxically increased Cox-2 expression in veh-treated mice. Cox-2 is capable of producing both pro- and anti-inflammatory mediators, and AT-RvD1 has been shown to increase Cox-2 under homeostatic conditions in human macrophages (20, 41). Therefore, AT-RvD1 may be acting to promote other SPMs or PGs to maintain homeostatic conditions in the absence of an inflammatory response, but dampening NTHi-induced Cox-2 expression to prevent production of proinflammatory mediators. Furthermore, PGE_2 continues to increase at 24 h, in contrast to other cytokines, despite no change in mouse PGE synthase 1 (data not shown). Although Cox-2 expression is lower at 24 h than at 6 h, Cox-2 in veh/NTHi mice is still significantly elevated above that in veh/veh mice, which could account for the increased PGE_2. Furthermore, PGE_2 has been shown to have both pro- and anti-inflammatory actions. Thus, late-stage PGE_2 could be acting in an anti-inflammatory manner or may simply be the result of accumulated PGs. The connection between Cox-2 and SPM production is a broad area of study and one that bears further investigation in this model. Overall, regulation of lipid mediator class switching is an important characteristic of SPMs, as is the shift to promote anti-inflammatory cytokines. Eicosanoids, including both SPMs and proinflammatory mediators, produced in the early stages of inflammation can form feedback loops to promote the shift to

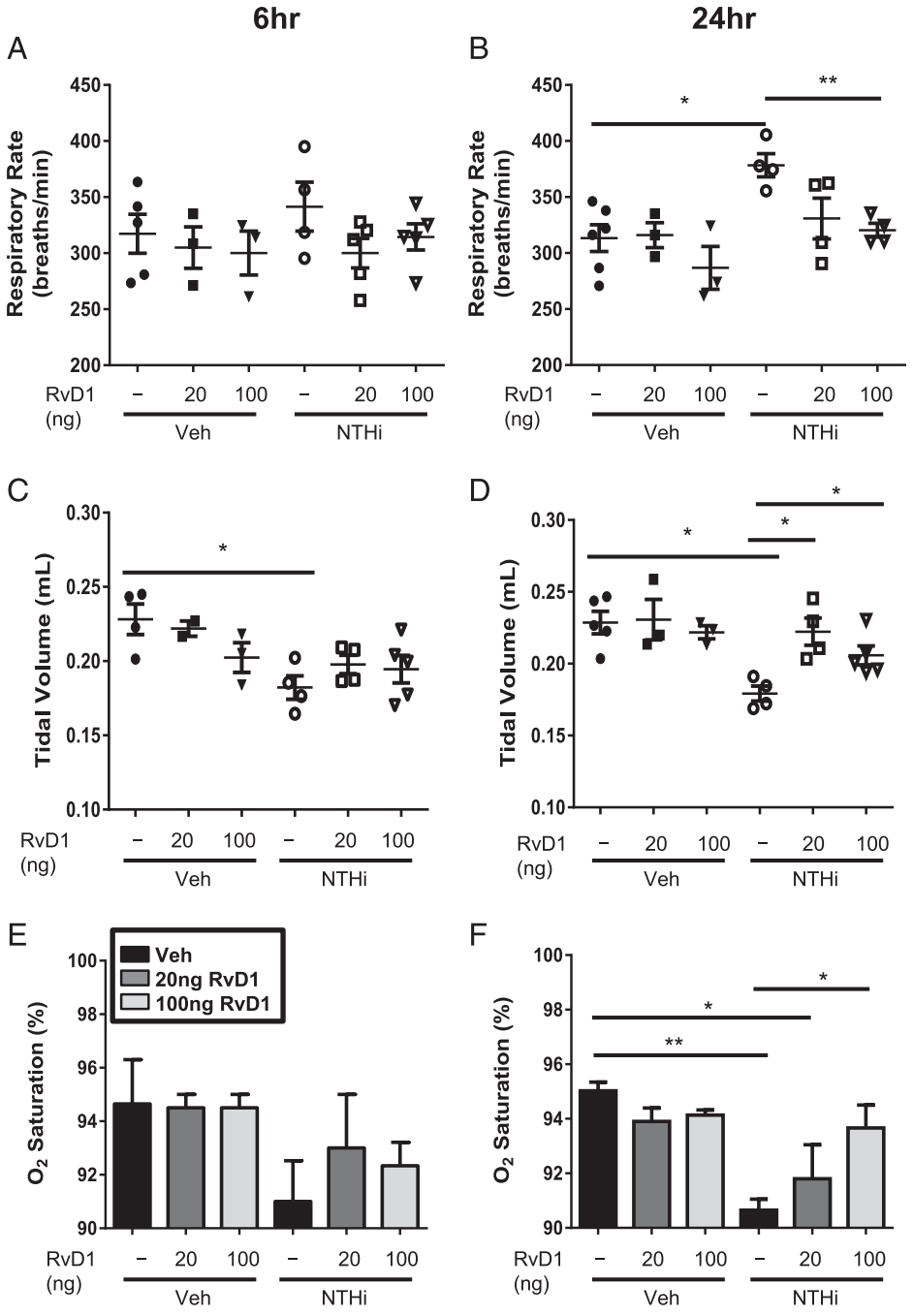

FIGURE 8. AT-RvD1 improves respiratory health in NTHi-infected mice. Respiratory outcomes were measured for mice inoculated with AT-RvD1 (veh, black bars; 20 ng per mouse, dark gray bars; or 100 ng per mouse, light gray bars, oropharyngeal aspiration) and/or NTHi (1×10^6 CFUs, oropharyngeal aspiration) at 6 and 24 h post infection. Respiratory rates (**A** and **B**), tidal volume (**C** and **D**), and O_2 saturation of hemoglobin (**E** and **F**) were assessed. Statistical significance was determined by two-way ANOVA. Overall $p = 0.0044$, NTHi (B), $p = 0.004$, NTHi (C), $p = 0.002$ (D), $p = 0.0005$, NTHi (F), $p = 0.0069$, AT-RvD1 (B), $p = 0.0452$, AT-RvD1 (D) with the Bonferroni posttest for multiple comparisons (*$p < 0.05$, **$p < 0.01$), $n = 3$–6 mice per group.

anti-inflammatory lipids (40, 42). Although further in-depth investigations are needed to fully elucidate the role of Cox-2 in inflammation and SPM-mediated resolution, there is evidence that these distinct lipid mediator profiles produced at different stages of inflammation can mediate the progression from initiation of inflammation through to resolution and can reprogram immune cells to promote resolution.

In our studies, some actions of AT-RvD1 are dose dependent (such as phagocytosis and efferocytosis), whereas other effects are similar at the 20-ng and 100-ng doses (such as reductions in inflammatory cells and cytokines). Different components of the resolution process may be more sensitive to the actions of AT-RvD1 (such as dampening of inflammatory cytokines compared with proresolving phagocytosis), and it is possible that a dose-dependent change in cytokines and inflammatory cells would have been seen at doses <20 ng. Because different SPMs act through different receptors (43, 44), it is also possible that a combination of SPMs would have stronger proresolving effects than higher doses of single SPMs. Such combination studies will be an important next step toward development of SPMs as clinical therapies.

The non-immunosuppressive properties of SPMs are most clearly demonstrated by their ability to mediate macrophage phenotypic switching. We observed an increase in the percentage of M2 macrophages and a decrease in the percentage of M1 macrophages, culminating in an overall shift in the ratio of these phenotypes with AT-RvD1 treatment. M2 macrophages are known to promote resolution, and a number of studies have demonstrated their enhanced phagocytic capabilities (39, 45–47). Moreover, multiple chronic inflammatory diseases have been linked to a skewed M1/M2 profile, with a deficiency in M2 macrophages presumably causing phagocytic and resolution deficiencies (45, 48).

Patients with COPD in particular have deficient phagocytosis, and NTHi is a common pathogen in COPD exacerbations and other underlying inflammatory conditions (3). NTHi can avoid opsonization and clearance, allowing for persistent colonization in the human lung. In our study, AT-RvD1 increased bacterial clearance from the lung through enhanced macrophage phagocytosis. Although the specific mechanisms by which AT-RvD1 acts to enhance phagocytosis are unknown, this ability has been observed in other models (20–22, 38). In addition, AT-RvD1–treated mice may have decreased bacterial burden because of enhanced macrophage killing. Although SPMs do not have direct antibacterial properties, they can enhance internalization of bacteria, TNF-α expression, and reactive oxygen species production to mediate killing (25, 33). Although we have not yet demonstrated that AT-RvD1 or other SPMs can improve phagocytosis and bacterial killing in the context of chronic lung inflammatory disease, we recently reported that AT-RvD1 attenuates cigarette smoke–induced emphysema in a mouse model, with reductions in inflammatory signaling and oxidative stress (49). Future studies that evaluate SPMs in a setting of infection following chronic lung disease will be important to understand the translation potential of these compounds. We will also be very interested to determine whether SPMs are equally efficacious in a model of chronic recurrent infection—that is, whether SPMs would be effective if given during a third or fourth infection after several rounds of untreated infection.

AT-RvD1 may be acting through a number of signaling pathways to mediate its effects. As described above, Cox-2 can regulate the production of pro- and anti-inflammatory signals, including SPM production. NTHi has been shown to activate the NF-κB and MAPK pathways to promote inflammation (17). SPMs have also been shown in multiple studies to act on the NF-κB pathway to mediate their effects (20, 24, 27, 33). Moreover, NTHi induces expression of TAK-1, which leads to enhanced NF-κB expression; TAK-1 is negatively regulated by cylindromatosis (CYLD), a primary negative regulator for NTHi-induced inflammation overall (50, 51). Our laboratory has shown in epithelial cells that AT-RvD1 can dampen TAK-1, highlighting another potential target in NTHi infections (37). Many different signaling molecules exist that are regulated by both NTHi and SPMs, and these candidate markers represent an interesting area for future mechanistic studies.

The proresolving actions of AT-RvD1 yielded markedly improved respiratory physiology in treated mice in this study. NTHi-infected mice demonstrated elevated respiratory rates and decreased tidal volumes; importantly, these alterations were accompanied by dramatic decreases in oxygen saturation of hemoglobin, highlighting an important clinical consequence of impaired lung physiology. Remarkably, AT-RvD1 treatment significantly improved lung physiology, resulting in improved oxygen saturation of hemoglobin in NTHi-infected mice. The ability of AT-RvD1 to protect against NTHi-induced weight loss was likely multifactorial; because treated mice had improved respiratory physiology and thermal homeostasis, and thus lower metabolic demand for basic functions such as breathing and maintaining body temperature, this contributed to preventing weight loss. These are the first observed effects of NTHi on respiratory rates, oxygen saturation, and temperature in mice, and the first evidence that SPMs can act to improve these health markers in a live bacteria, pulmonary infection model.

These data represent, to our knowledge, the first evidence in a pulmonary model that SPMs can act in a proresolving manner to dampen inflammation and improve lung physiology while still enhancing bacterial clearance. These unique properties open up a wide range of therapeutic opportunities for AT-RvD1, particularly as an alternative for chronic inflammatory conditions such as COPD, in which infective exacerbations are common. AT-RvD1 has high therapeutic potential for such patients, and these studies are a step in investigating this novel and critical area of resolution research.

Acknowledgments

We thank the University of Rochester Medical Center Vivarium for providing instruments for several animal procedures; the University of Rochester Medical Center flow core for flow cytometry assistance; the Jian-Dong Li laboratory for generous donation of NTHi; Kristina Owens, Claire McCarthy, and Parker Duffney for technical assistance; and Samir Bhagwat, Frank Gigliotti, and Terry Wright for technical expertise and use of equipment in measuring respiratory outcomes and O_2 saturation.

Disclosures

The authors have no financial conflicts of interest.

References

1. Murphy, T. F. 2005. Haemophilus Infections. In *Harrison's Principles of Internal Medicine.* F. Braunwald, D. L. Kaspar, S. L. Hauser, D. L. Longo, and L. Jameson, eds. McGraw Hill, New York, NY, p. 939–942.
2. King, P. T., and R. Sharma. 2015. The lung immune response to nontypeable *Haemophilus influenzae* (lung immunity to NTHi). *J. Immunol. Res.* 2015: 706376.
3. Moghaddam, S. J., C. E. Ochoa, S. Sethi, and B. F. Dickey. 2011. Nontypeable *Haemophilus influenzae* in chronic obstructive pulmonary disease and lung cancer. *Int. J. Chron. Obstruct. Pulmon. Dis.* 6: 113–123.
4. King, P. T., S. R. Holdsworth, N. J. Freezer, E. Villanueva, and P. W. Holmes. 2007. Microbiologic follow-up study in adult bronchiectasis. *Respir. Med.* 101: 1633–1638.
5. Fitzpatrick, M. E., S. Sethi, C. L. Daley, P. Ray, J. M. Beck, and M. R. Gingo. 2014. Infections in "noninfectious" lung diseases. *Ann. Am. Thorac. Soc.* 11(Suppl 4): S221–S226.
6. Bandi, V., M. A. Apicella, E. Mason, T. F. Murphy, A. Siddiqi, R. L. Atmar, and S. B. Greenberg. 2001. Nontypeable *Haemophilus influenzae* in the lower respiratory tract of patients with chronic bronchitis. *Am. J. Respir. Crit. Care Med.* 164: 2114–2119.
7. Desai, H., K. Eschberger, C. Wrona, L. Grove, A. Agrawal, B. Grant, J. Yin, G. I. Parameswaran, T. Murphy, and S. Sethi. 2014. Bacterial colonization increases daily symptoms in patients with chronic obstructive pulmonary disease. *Ann. Am. Thorac. Soc.* 11: 303–309.
8. Bandi, V., M. Jakubowycz, C. Kinyon, E. O. Mason, R. L. Atmar, S. B. Greenberg, and T. F. Murphy. 2003. Infectious exacerbations of chronic obstructive pulmonary disease associated with respiratory viruses and nontypeable *Haemophilus influenzae. FEMS Immunol. Med. Microbiol.* 37: 69–75.
9. Hurst, J. R., J. Vestbo, A. Anzueto, N. Locantore, H. Müllerova, R. Tal-Singer, B. Miller, D. A. Lomas, A. Agusti, W. Macnee, et al; Evaluation of COPD Longitudinally to Identify Predictive Surrogate Endpoints (ECLIPSE) Investigators. 2010. Susceptibility to exacerbation in chronic obstructive pulmonary disease. *N. Engl. J. Med.* 363: 1128–1138.
10. Centers for Disease Control and Prevention. 2013. Active bacterial core surveillance report, emerging infections program network, *Haemophilus influenza* 2013. Available at: http://www.cdc.gov/abcs/reports-findings/survreports/hi13.pdf.
11. Resman, F., M. Ristovski, A. Forsgren, B. Kaijser, G. Kronvall, P. Medstrand, E. Melander, I. Odenholt, and K. Riesbeck. 2012. Increase of β-lactam-resistant invasive *Haemophilus influenzae* in Sweden, 1997 to 2010. *Antimicrob. Agents Chemother.* 56: 4408–4415.
12. Wan Sai Cheong, J., H. Smith, C. Heney, J. Robson, S. Schlebusch, J. Fu, and C. Nourse. 2015. Trends in the epidemiology of invasive *Haemophilus influenzae* disease in Queensland, Australia from 2000 to 2013: what is the impact of an increase in invasive non-typable *H. influenzae* (NTHi)? *Epidemiol. Infect.* 143: 2993–3000.
13. Clementi, C. F., and T. F. Murphy. 2011. Non-typeable *Haemophilus influenzae* invasion and persistence in the human respiratory tract. *Front. Cell. Infect. Microbiol.* 1: 1.
14. Hallström, T., and K. Riesbeck. 2010. *Haemophilus influenzae* and the complement system. *Trends Microbiol.* 18: 258–265.
15. Lugade, A. A., P. N. Bogner, T. F. Murphy, and Y. Thanavala. 2011. The role of TLR2 and bacterial lipoprotein in enhancing airway inflammation and immunity. *Front. Immunol.* 2: 10.
16. Lugade, A. A., R. R. Vethanayagam, M. Nasirikenari, P. N. Bogner, B. H. Segal, and Y. Thanavala. 2011. Nrf2 regulates chronic lung inflammation and B-cell responses to nontypeable *Haemophilus influenzae. Am. J. Respir. Cell Mol. Biol.* 45: 557–565.
17. Xu, F., Z. Xu, R. Zhang, Z. Wu, J. H. Lim, T. Koga, J. D. Li, and H. Shen. 2008. Nontypeable *Haemophilus influenzae* induces COX-2 and PGE2 expression in lung epithelial cells via activation of p38 MAPK and NF-kappa B. *Respir. Res.* 9: 16.

18. Xu, X., R. R. Steere, C. A. Fedorchuk, J. Pang, J. Y. Lee, J. H. Lim, H. Xu, Z. K. Pan, S. B. Maggirwar, and J. D. Li. 2011. Activation of epidermal growth factor receptor is required for NTHi-induced NF-κB-dependent inflammation. *PLoS One* 6: e28216.
19. Buckley, C. D., D. W. Gilroy, and C. N. Serhan. 2014. Proresolving lipid mediators and mechanisms in the resolution of acute inflammation. *Immunity* 40: 315–327.
20. Croasdell, A., T. H. Thatcher, R. M. Kottmann, R. A. Colas, J. Dalli, C. N. Serhan, P. J. Sime, and R. P. Phipps. 2015. Resolvins attenuate inflammation and promote resolution in cigarette smoke-exposed human macrophages. Am. J. Physiol. Lung Cell. Mol. Physiol. 309: L888–L991.
21. Hsiao, H. M., R. E. Sapinoro, T. H. Thatcher, A. Croasdell, E. P. Levy, R. A. Fulton, K. C. Olsen, S. J. Pollock, C. N. Serhan, R. P. Phipps, and P. J. Sime. 2013. A novel anti-inflammatory and pro-resolving role for resolvin D1 in acute cigarette smoke-induced lung inflammation. *PLoS One* 8: e58258.
22. Dalli, J., and C. N. Serhan. 2012. Specific lipid mediator signatures of human phagocytes: microparticles stimulate macrophage efferocytosis and pro-resolving mediators. *Blood* 120: e60–e72.
23. Rogerio, A. P., O. Haworth, R. Croze, S. F. Oh, M. Uddin, T. Carlo, M. A. Pfeffer, R. Priluck, C. N. Serhan, and B. D. Levy. 2012. Resolvin D1 and aspirin-triggered resolvin D1 promote resolution of allergic airways responses. *J. Immunol.* 189: 1983–1991.
24. Liao, Z., J. Dong, W. Wu, T. Yang, T. Wang, L. Guo, L. Chen, D. Xu, and F. Wen. 2012. Resolvin D1 attenuates inflammation in lipopolysaccharide-induced acute lung injury through a process involving the PPARγ/NF-κB pathway. *Respir. Res.* 13: 110.
25. Palmer, C. D., C. J. Mancuso, J. P. Weiss, C. N. Serhan, E. C. Guinan, and O. Levy. 2011. 17(R)-Resolvin D1 differentially regulates TLR4-mediated responses of primary human macrophages to purified LPS and live *E. coli*. *J. Leukoc. Biol.* 90: 459–470.
26. Kure, I., S. Nishiumi, Y. Nishitani, T. Tanoue, T. Ishida, M. Mizuno, T. Fujita, H. Kutsumi, M. Arita, T. Azuma, and M. Yoshida. 2010. Lipoxin A(4) reduces lipopolysaccharide-induced inflammation in macrophages and intestinal epithelial cells through inhibition of nuclear factor-kappaB activation. *J. Pharmacol. Exp. Ther.* 332: 541–548.
27. Chen, F., X. H. Fan, Y. P. Wu, J. L. Zhu, F. Wang, L. L. Bo, J. B. Li, R. Bao, and X. M. Deng. 2013. Resolvin D1 improves survival in experimental sepsis through reducing bacterial load and preventing excessive activation of inflammatory response. *Eur J. Clin. Microbiol. Infect. Dis.* 33: 457–464.
28. Walker, J., E. Dichter, G. Lacorte, D. Kerner, B. Spur, A. Rodriguez, and K. Yin. 2011. Lipoxin a4 increases survival by decreasing systemic inflammation and bacterial load in sepsis. *Shock* 36: 410–416.
29. Spite, M., L. V. Norling, L. Summers, R. Yang, D. Cooper, N. A. Petasis, R. J. Flower, M. Perretti, and C. N. Serhan. 2009. Resolvin D2 is a potent regulator of leukocytes and controls microbial sepsis. *Nature* 461: 1287–1291.
30. Abdulnour, R. E., H. P. Sham, D. N. Douda, R. A. Colas, J. Dalli, Y. Bai, X. Ai, C. N. Serhan, and B. D. Levy. 2015. Aspirin-triggered resolvin D1 is produced during self-resolving gram-negative bacterial pneumonia and regulates host immune responses for the resolution of lung inflammation. *Mucosal Immunol.*
31. Gobbetti, T., S. M. Coldewey, J. Chen, S. McArthur, P. le Faouder, N. Cenac, R. J. Flower, C. Thiemermann, and M. Perretti. 2014. Nonredundant protective properties of FPR2/ALX in polymicrobial murine sepsis. *Proc. Natl. Acad. Sci. USA* 111: 18685–18690.
32. Wu, B., J. A. Walker, D. Temmermand, K. Mian, B. Spur, A. Rodriguez, T. P. Stein, P. Banerjee, and K. Yin. 2013. Lipoxin A(4) promotes more complete inflammation resolution in sepsis compared to stable lipoxin A(4) analog. *Prostaglandins Leukot. Essent. Fatty Acids* 89: 47–53.
33. Chiang, N., G. Fredman, F. Bäckhed, S. F. Oh, T. Vickery, B. A. Schmidt, and C. N. Serhan. 2012. Infection regulates pro-resolving mediators that lower antibiotic requirements. *Nature* 484: 524–528.
34. Ueda, T., K. Fukunaga, H. Seki, J. Miyata, M. Arita, T. Miyasho, T. Obata, K. Asano, T. Betsuyaku, and J. Takeda. 2014. Combination therapy of 15-epi-lipoxin A4 with antibiotics protects mice from *Escherichia coli*-induced sepsis*. *Crit. Care Med.* 42: e288–e295.
35. Lakatos, H. F., H. A. Burgess, T. H. Thatcher, M. R. Redonnet, E. Hernady, J. P. Williams, and P. J. Sime. 2006. Oropharyngeal aspiration of a silica suspension produces a superior model of silicosis in the mouse when compared to intratracheal instillation. *Exp. Lung Res.* 32: 181–199.
36. McMillan, D. H., C. J. Baglole, T. H. Thatcher, S. Maggirwar, P. J. Sime, and R. P. Phipps. 2011. Lung-targeted overexpression of the NF-κB member RelB inhibits cigarette smoke-induced inflammation. *Am. J. Pathol.* 179: 125–133.
37. Hsiao, H. M., T. H. Thatcher, E. P. Levy, R. A. Fulton, K. M. Owens, R. P. Phipps, and P. J. Sime. 2014. Resolvin D1 attenuates polyinosinic-polycytidylic acid-induced inflammatory signaling in human airway epithelial cells via TAK1. *J. Immunol.* 193: 4980–4987.
38. Colas, R. A., M. Shinohara, J. Dalli, N. Chiang, and C. N. Serhan. 2014. Identification and signature profiles for pro-resolving and inflammatory lipid mediators in human tissue. *Am. J. Physiol. Cell Physiol.* 307: C39–C54.
39. Ariel, A., and C. N. Serhan. 2012. New lives given by cell death: macrophage differentiation following their encounter with apoptotic leukocytes during the resolution of inflammation. *Front. Immunol.* 3: 4.
40. Levy, B. D., C. B. Clish, B. Schmidt, K. Gronert, and C. N. Serhan. 2001. Lipid mediator class switching during acute inflammation: signals in resolution. *Nat. Immunol.* 2: 612–619.
41. Gilroy, D. W., P. R. Colville-Nash, D. Willis, J. Chivers, M. J. Paul-Clark, and D. A. Willoughby. 1999. Inducible cyclooxygenase may have anti-inflammatory properties. *Nat. Med.* 5: 698–701.
42. Wu, D., S. Zheng, W. Li, L. Yang, Y. Liu, X. Zheng, Y. Yang, L. Yang, Q. Wang, F. G. Smith, and S. Jin. 2013. Novel biphasic role of resolvin D1 on expression of cyclooxygenase-2 in lipopolysaccharide-stimulated lung fibroblasts is partly through PI3K/AKT and ERK2 pathways. *Mediators Inflamm.* 2013: 964012.
43. Krishnamoorthy, S., A. Recchiuti, N. Chiang, S. Yacoubian, C. H. Lee, R. Yang, N. A. Petasis, and C. N. Serhan. 2010. Resolvin D1 binds human phagocytes with evidence for proresolving receptors. *Proc. Natl. Acad. Sci. USA* 107: 1660–1665.
44. Chiang, N., C. N. Serhan, S. E. Dahlén, J. M. Drazen, D. W. Hay, G. E. Rovati, T. Shimizu, T. Yokomizo, and C. Brink. 2006. The lipoxin receptor ALX: potent ligand-specific and stereoselective actions in vivo. *Pharmacol. Rev.* 58: 463–487.
45. Martinez, F. O., and S. Gordon. 2014. The M1 and M2 paradigm of macrophage activation: time for reassessment. *F1000Prime Rep.* 6: 13.
46. Titos, E., B. Rius, A. González-Périz, C. López-Vicario, E. Morán-Salvador, M. Martínez-Clemente, V. Arroyo, and J. Clària. 2011. Resolvin D1 and its precursor docosahexaenoic acid promote resolution of adipose tissue inflammation by eliciting macrophage polarization toward an M2-like phenotype. *J. Immunol.* 187: 5408–5418.
47. Martinez, F. O., A. Sica, A. Mantovani, and M. Locati. 2008. Macrophage activation and polarization. *Front. Biosci.* 13: 453–461.
48. Hodge, S., G. Matthews, V. Mukaro, J. Ahern, A. Shivam, G. Hodge, M. Holmes, H. Jersmann, and P. N. Reynolds. 2011. Cigarette smoke-induced changes to alveolar macrophage phenotype and function are improved by treatment with procysteine. *Am. J. Respir. Cell Mol. Biol.* 44: 673–681.
49. Hsiao, H. M., T. H. Thatcher, R. A. Colas, C. N. Serhan, R. P. Phipps, and P. J. Sime. 2015. Resolvin D1 reduces emphysema and chronic inflammation. *Am. J. Pathol.* 185: 3189–3201.
50. Lim, J. H., H. Jono, T. Koga, C. H. Woo, H. Ishinaga, P. Bourne, H. Xu, U. H. Ha, H. Xu, and J. D. Li. 2007. Tumor suppressor CYLD acts as a negative regulator for non-typeable *Haemophilus* influenza-induced inflammation in the middle ear and lung of mice. *PLoS One* 2: e1032.
51. Kovalenko, A., C. Chable-Bessia, G. Cantarella, A. Israël, D. Wallach, and G. Courtois. 2003. The tumour suppressor CYLD negatively regulates NF-kappaB signalling by deubiquitination. *Nature* 424: 801–805.